

Indirect imaging of polars

A.D. SCHWOPE¹, A. STAUDE¹, J. VOGEL¹, and R. SCHWARZ²

¹ Astrophysikalisches Institut Potsdam, An der Sternwarte 16, 14482 Potsdam, Germany

² Universitäts-Sternwarte Göttingen, Geismarlandstr. 11, 37083 Göttingen, Germany

Received 6 October 2003; accepted 2 December 2003; published online 29 February 2004

Abstract. Tomographic techniques of different flavour offer enormous diagnostic power for the analysis of magnetic cataclysmic binaries, particularly those of AM Herculis type, the so-called *polars*. The three main ingredients of such systems, the donor star, the accretor and the accretion stream between the two stars, are investigated by Doppler tomography, Roche tomography and eclipse mapping methods. The indirect imaging methods reveal the structure, extent and ionization conditions in the accretion stream, they reveal the extent of the irradiation zone on the secondary star and constrain the mass ratio and the orbital inclination of the binary. We describe a new code for Roche tomography, the achievements and limitations of straight Doppler tomography and a new mapping technique tentatively called curtain tomography. This new technique will map emission line profiles to an accretion curtain making full use of the velocity and the photometric information.

Key words: cataclysmic variables – methods: data analysis

©2004 WILEY-VCH Verlag GmbH & Co. KGaA, Weinheim

1. Introduction

The typical polar is a short-period cataclysmic variable with a late-type secondary star as donor (M3 or later) and a magnetic white dwarf, $B = 10 - 200$ MG, accreting via an accretion stream. The strong magnetic field of the white dwarf keeps both stars in rigid rotation, prevents the formation of an accretion disk and causes intensive cyclotron radiation from the accretion hot spot(s). The accreting spots are otherwise the sources of hard, bremsstrahlung-like, X-ray radiation from the cooling, shocked plasma and of soft X-rays from the heated atmosphere.

The presence of mainly one period, the orbital period, together with a relatively simple geometry makes those systems well-suited for indirect imaging techniques, despite their relative faintness and their short periods. The donor star is studied by straight Doppler tomography (e.g. Schwöpe et al. 2000) and Roche tomography (Watson et al. 2003 and this volume). The white dwarf is studied by eclipse mapping of the accretion hot spot (e.g. Gänsicke et al. 1998), Stokes imaging (Potter et al. 1998) and Zeeman imaging (Euchner et al. 2002). The latter two refer to the magnetism of the white dwarf, which manifests itself in cyclotron emission from the accretion spot and photospheric Zeeman absorption from the whole surface. The accretion stream finally is studied by

Doppler tomography (e.g. Schwöpe et al. 1997) and several flavours of accretion stream mapping (ASM: Hakala 1995, Harrop-Allin et al. 1999, Kube et al. 2000, Vriellmann & Schwöpe 2001). The ASM-techniques are derivatives of classical eclipse mapping making use of either the eclipses of the stream by the donor or by the stream itself.

In this short review we are describing the main achievements of indirect imaging techniques of the secondary star and the accretion stream.

2. Roche tomography

Roche-tomography (Rutten & Dhillon 1994) determines the brightness distribution on the Roche-lobe of the secondary star. A least-squares fit is combined with a smoothness criterion to map a trailed spectrogram of either emission or absorption lines to a pre-defined structure in the 6-dimensional phase space (r, v). The intrinsic line-profile is assumed to be the same for all surface elements, i.e. all broadening in an observed spectrum is ascribed to Doppler-shifts.

In our code, the smoothness is accounted for using a Maximum Entropy (MEM) approach. Any intrinsic line-profile can be used. Watson & Dhillon (2001) explored the artefacts generated by reconstructions with a false limb-darkening law. They used as reference a conventional power-law model. Orosz & Hauschildt (2000) and more recently Hadrava & Kubat (2003) have shown that continuum and absorption

Correspondence to: ASchwöpe@aip.de

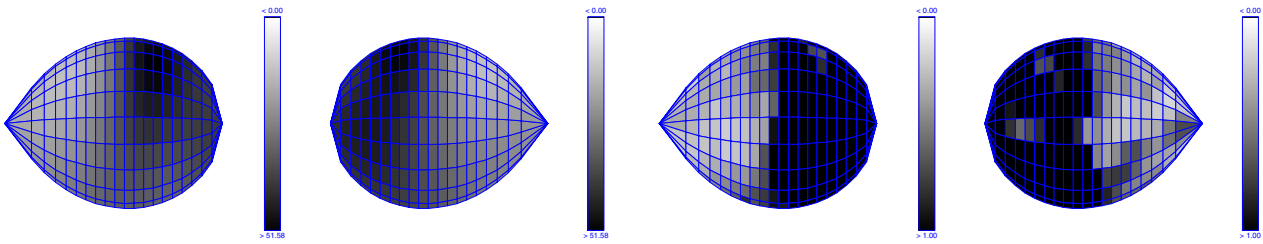


Fig. 1. (online colour at: www.interscience.wiley.com) (left) The Na-map of AM Her for $Q = 1.0$, $M_1 = 0.46 M_\odot$, and $i = 58^\circ$, shown at phases 0.25 and 0.75 at $i = 58^\circ$. (Intensity in arbitrary units. Black denotes maximum intensity, white zero intensity.) (right) The significance map for the best fit Roche map at the same phases as in the left two diagrams. It is calculated with respect to the average value of the unirradiated hemisphere. Values below 1 (i.e. brighter than black) denote that the features in the data map are significant with respect to the comparison level, i.e. the depletion on the irradiated hemisphere is real.

line limb-darkening is not well described by the ‘established’ power laws. Even more, absorption lines may develop emission wings when observed at the stellar limb. Instead of using a wrong law we decided not to use any limb-darkening in the present version of the code. This seems to be *post factum* justified by the fact, that our maps do not show any sign of the possible residuals as described in Watson & Dhillon (2001).

The quality of the fit is the sum of the χ^2 of the fit and the entropy, weighted by a user-specified parameter, which controls the importance of the smoothness for the quality determination. The entropy is calculated with respect to a default-map, which is a smoothed version of the actual data-map.

Our code uses Evolution Strategy to reach the minimum χ^2 of the fit (Rechenberg 1973). This method uses an adaptation scheme of mutation and selection for breeding children (modified maps) from a parent population. The best-fitting individuals have a higher probability to inherit their attributes to the next generation, the less suited ones die out. By applying random variations to the brightness map the probability to get stuck within a local minimum is lower than in fully deterministic optimisation techniques. However, in contrast to Monte-Carlo methods the modifications are not completely arbitrary and the results of earlier generations are the basis for further improvements.

The actual fitting is done in the following way: Starting with an initial map the quality of the fit is determined. An iterative process then modifies the map until the χ^2 reaches a predefined value and then tries to maximise the entropy until the maximum number of iterations (defined sufficiently high) is exceeded.

In order to estimate how much of the structure seen in the maps is real and not just *one* representation of multiple possibilities to fit the data, we use a version of the bootstrap method described by Watson & Dhillon (2001) which yields a significance map (Fig. 1).

The whole method relies on the assumption that the smoothest map represents the true system parameters of the binary, i.e. these can be determined by exploring the entropy landscape as a function of the inclination i , the mass ratio $Q = M_1/M_2$, and the mass of the white dwarf M_1 . Watson et al. (2003) already used this approach to deter-

mine the system parameters of AM Her, leading to values of $q = M_2/M_1 = 0.53$, $M_1 = 0.36 M_\odot$, and $i = 60 - 80^\circ$.

AM Her was observed on August 4, 5 and 6, 2000 at the 3.5m-telescope at Calar Alto, Spain, with the two-channel spectrograph TWIN. Around the sodium lines at 8183/8194 Å we achieved a spectral resolution of 1.4 Å (see Fig. 2 and Staude et al. 2003). A grid of parameter combinations from $Q = 0.5 \dots 1.5$ (stepsize 0.1), $M_1 = 0.1 \dots 1.0 M_\odot$ (stepsize 0.09), and $i = 30 \dots 70^\circ$ (stepsize 4°) was computed. The entropy was calculated with respect to a smoothed version of the actual data map. The smoothest map at $\chi^2 = 0.25$ was found to be the one at $Q = 1.0$, $M_1 = 0.46 M_\odot$, and $i = 58^\circ$ (shown in Fig. 1). The resulting spectra and the residuals are also shown in Fig. 2. The bootstrap test (Fig. 1, right) shows that the only significant feature in the map is the Na-depletion on the irradiated hemisphere of the donor star. Any further substructure on the two half-spheres is insignificant with the present level of accuracy and signal-to-noise of the input data. We mention in particular, that no pronounced left-right asymmetry seems to be present which would indicate significant shielding of (typically) the leading hemisphere due to absorbing material. The likely cause for the obvious difference of our best-fit param-

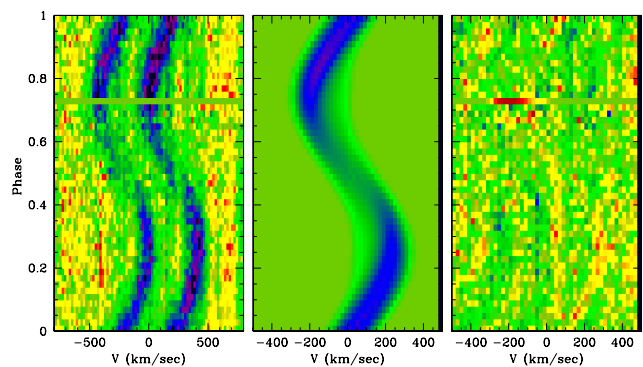


Fig. 2. (online colour at: www.interscience.wiley.com) left: The phase-folded, averaged, sodium lines of AM Her, obtained August 4–6, 2000. The continuum emission is subtracted. middle: best fit to the data, the projection of only one line is shown. right: residuals of the fit, all representations use the same high and low cuts.

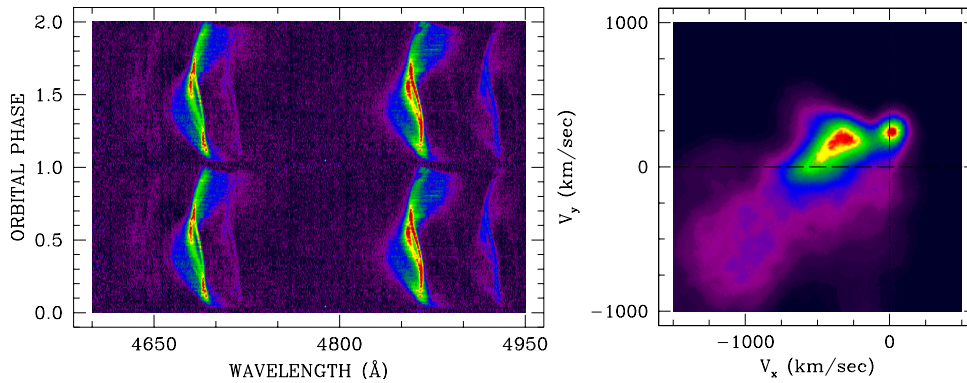


Fig. 3. (online colour at: www.interscience.wiley.com) (left) Phase-folded, continuum-subtracted trailed spectrogram of HU Aqr, obtained in a low accretion state. Phase-bins correspond to 1.25 min of the $P_{\text{orb}} = 125$ min binary, the spectral resolution is 0.5 Å. The bright lines belong to He II $\lambda 4686$, H β , and He I $\lambda 4921$. The same data are shown twice for clarity. (right) Doppler map of the He II $\lambda 4686$ line.

eters with respect to the Watson et al. values needs to be explored.

3. Doppler tomography

Straight Doppler tomography of emission lines of polars, particularly of high-inclination systems, may reveal a basic understanding of the complex emission line profiles, as shown in Fig. 3. Broadly speaking, under lucky circumstances the irradiated front side of the donor, the ballistic stream (or a kind of) and the magnetically guided part of the stream can be identified as separate structures in a high-quality Doppler map (see e.g. Schwobe et al. 1997, 2000, Fig. 3b shows the Doppler map of HU Aqr of the He II $\lambda 4686$ line in a low accretion state – the irradiated secondary and the magnetically guided part of the stream are clearly resolved). Based on these features, the extent of the ballistic stream, the orientation of the magnetic stream and the shielding of the donor star by an accretion curtain could be derived or inferred. This was fortunately possible, despite several basic assumptions of Doppler tomography being violated. Neither do we have velocity components only parallel to the orbital plane, nor is the source of light constant throughout the orbital cycle nor are all points equally visible at all phases.

However, only a few systems display easily understandable tomograms, and even those are far from being really understood. In HU Aqr, the 'ballistic' stream is much broader in v_y than compatible with supersonic motion alone (Heerlein et al. 1999). Compared with the prediction for the most likely value of the mass ratio of the binary, the stream is also displaced in negative v_y direction (Schwobe et al. 1997). In two Doppler maps of QQ Vul obtained at different epochs, the ballistic stream appears displaced in v_y (Schwobe et al. 2000). AM Her showed a, nightly variable, distinct emission feature in the upper left quadrant outside the region of any simple model of the accretion geometry (Staude et al. 2003). At another occasion it showed a spot of emission at zero velocity just below the L_1 (Gänsicke et al. 1998). Both observations are likely to be connected with the magnetic activity and magnetic field of the secondary star. Other systems, even high-inclination systems like V1309 Ori, do not show any sign of a ballistic stream as a separate structure at all (Staude et al. 2001).

4. Accretion stream/Curtain mapping

The complications described and the high photometric variability of the emission lines triggered several attempts of accretion stream mapping (ASM). In the present flavours of ASM a light curve is mapped on an accretion stream, usually divided in two parts, the first part follows a ballistic trajectory, the second, magnetic part, is determined by a dipolar field line connecting the stagnation region with the white dwarf surface. The methods differ in the type of input data, the phase coverage of such data and the geometry of the stream. They concentrate mainly on the two twin systems, HU Aqr and UZ For, due to their preferred geometry. Hakala (1995) and Harrop-Allin et al. (1999) used a short interval of broad-band UBVRI data, centered on the eclipse of the white dwarf. Such data have the advantage of high signal-to-noise ratio but suffer from strong and variable contamination from underlying radiation components. Kube et al. (1999) used the integrated line flux of the ultraviolet (HST/FOS) CIV lines of UZ For, again only a short time interval of data centered on the eclipse. Such data are well suited for mapping experiments since they have a good signal-to-noise and time resolution and are free from contaminating background components. However, out-of-eclipse photometric variability is evident in the spectral lines but neglected by those authors which limits the predictive power of their approach. Realizing that the strong orbital variability of optical emission lines in HU Aqr allows the application of classical eclipse mapping techniques, Vrielmann & Schwobe (2001) mapped emission line light curves with full phase coverage on a three-dimensional tube along the ballistic and a dipolar magnetic field line. Those data, clean of background contaminations, have lower signal-to-noise and time resolution than those mentioned above.

None of these attempts yield fully satisfactory and convincing results, nor do the results for the same system converge. While the method by Hakala & Harrop-Allin tends to emphasize the region close to the white dwarf, the Kube et al. maps show some bright regions on somewhat arbitrary regions on the stream and the Vrielmann & Schwobe attempt emphasizes the stagnation region. The latter seems physically reasonable, the predicted light curve at eclipse phase, however, is barely compatible with broad-band light curves obtained at the same time.

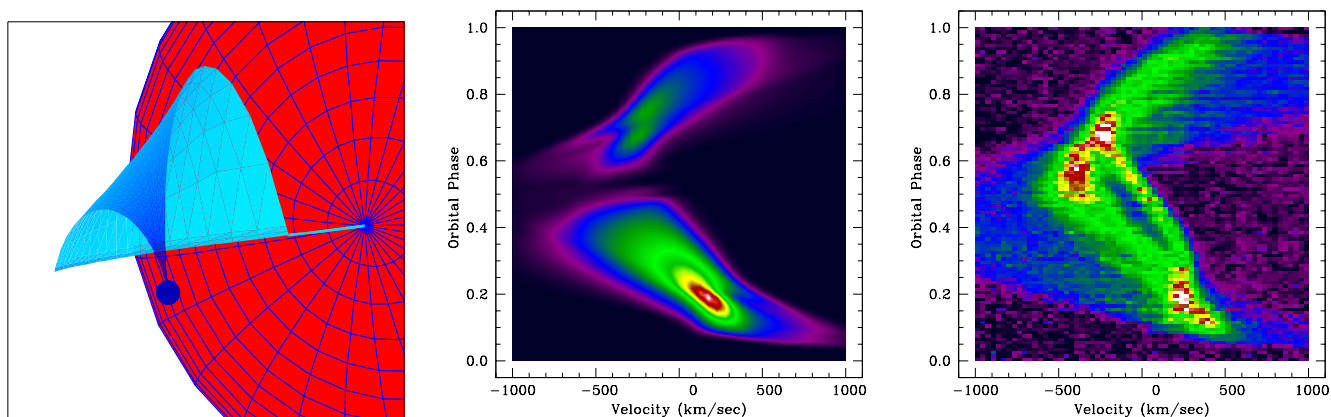


Fig. 4. (online colour at: www.interscience.wiley.com) (*left*) View of the accretion curtain in an HU Aqr-like geometry at binary phase 0.46. The colour of the curtain codes velocity, not brightness. (*middle*) Trailed spectrogram of emission from the ballistic stream and the accretion curtain in an HU Aqr-like geometry. The brightness distribution on each of the different parts of the stream is characterized by constant surface brightness plus fore-shortening factor with a contrast of 10:1 between the ballistic and magnetic part of the flow. (*right*) Trailed spectrogram of He II λ 4686 of HU Aqr (detail of Fig. 3).

Since some of the basic assumptions of Doppler-tomography are violated in polars and eclipse mapping methods disregard the velocity information, we attempt to combine both methods. We started to develop a code which maps a trailed spectrogram on an accretion curtain, or more general a structure in the 6-dimensional phase space.

In our model the accretion curtain is defined by dipolar fieldlines intersecting the ballistic stream, assuming a certain orientation of the magnetic axis. The azimuth of curtain begin and end are treated as free parameters. The curtain is dissected in triangular-shaped surface elements (tiles) whose size is determined mainly by the local velocity gradient. Its velocity is defined by the velocity of the center of mass of each tile. The ballistic stream is shaped as a n -sided tube. The initial v_{mag} is the velocity component parallel to the field lines at the coupling point. We handle the eclipsing events by a polygon intersection algorithm to be free in the choice of optical depth effects. Irradiation effects by the hot spot are included. Having set the magnetic geometry, the size of the curtain, and the orbital inclination (see Fig. 4 and movies in the online version), trailed spectra for arbitrary brightness distributions and optical depths can be calculated (for an example see Fig. 4). The model assumes an extent of the curtain between 4° and 44° in azimuth along the ballistic stream, an inclination of 85° , and an azimuth and colatitude of the dipolar axis of 45° and 12° , respectively. The curtain was optically thick, the brightness contrast between the magnetic and the ballistic stream was 1:10).

The current version of the code is a useful tool for investigating the influence of the different parameters (geometry, optical depth, brightness distribution, velocity field) on the predicted line profiles and the light curves. The next step – fitting the observed spectra and computation of an intensity map all along the accretion curtain – is in progress. We will pay particular attention to the self-eclipse of the accretion curtain and to the eclipse of the curtain by the donor star. The online version of the paper illustrates the changing viewing geometry and velocity pattern of an accretion curtain in

a one-pole and a two-pole accretion geometry (HU Aqr- and AM Her-like).

5. Outlook

In future, the two codes described here may be joined and thus give full account to the content of the trailed spectrogram data. With only a few exceptions, the line profiles of polars are superpositions of emission lines from the accretion flow/curtain and the irradiated hemisphere of the secondary star. Such mapping experiment would take full account of the irradiation and shielding pattern of the stream/curtain on the one hand and the donor star on the other hand.

Acknowledgements. We thank an anonymous referee for helpful comments. RSC is supported by the Deutsches Zentrum für Luft- und Raumfahrt (DLR) GmbH under grant number 50 OR 0206.

References

- Euchner, F., Jordan, S., Beuermann, K., Gänsicke, B.T., Hessman, F.V.: 2002, *A&A* 390, 633
- Gänsicke, B.T., Hoard, D.W., Beuermann, K., Sion, E.M., Szkody, P.: 1998, *A&A* 338, 933
- Hadrava, P., Kubat, J.: 2003, *ASP Conf. Ser.* 288, 149
- Hakala, P.: 1995, *A&A* 294, 164
- Harrop-Allin, M., Hakala, P., Cropper, M.: 1999, *MNRAS* 302, 362
- Heerlein, C., Horne, K., Schwöpe, A.D.: 1999, *MNRAS* 304, 145
- Kube, J., Gänsicke, B.T., Beuermann, K.: 2000, *A&A* 356, 490
- Orosz, J.A., Hauschildt, P.H.: 2000, *A&A* 364, 265
- Potter, S.B., Hakala, P.J., Cropper, M.: 1998, *MNRAS* 297, 1261
- Rechenberg, I.: 1973, *Evolutionsstrategie*, Fromman-Holzboog, Stuttgart
- Rutten, R.G.M., Dhillon, V.S.: 1994, *A&A* 288, 773
- Schwöpe, A.D., Catalan, M.S., Beuermann, K., Metzner, A., Steeghs, D., Smith, R.C.: 2000, *MNRAS* 313, 533
- Schwöpe, A.D., Mantel, K.-H., Horne, K.: 1997, *A&A* 319, 894
- Staude, A., Schwöpe, A.D., Schwarz, R.: 2001, *A&A* 374, 588
- Staude, A., Schwöpe, A.D., Hedelt, P., Rau, A., Schwarz, R.: 2004, *Proc. IAU Coll. 190, ASP Conf. Ser.*, in press
- Vriellmann, S., Schwöpe, A.D.: 2001, *MNRAS* 322, 269
- Watson, C.A., Dhillon, V.S.: 2001, *MNRAS* 326, 67
- Watson, C.A., Dhillon, V.S., Rutten, R.G.M., Schwöpe, A.D.: 2003, *MNRAS* 341, 129